



Fast prediction of chatter stability in milling process based on an updated numerical solution scheme

Yan Xia^{1,2} · Yi Wan³ · Jin Du^{1,2} · Peirong Zhang^{1,2} · Guosheng Su^{1,2}

Received: 14 December 2021 / Accepted: 5 November 2022 / Published online: 18 November 2022
© The Author(s), under exclusive licence to Springer-Verlag London Ltd., part of Springer Nature 2022

Abstract

The stability prediction is an effective approach to suppress the unstable milling process caused by the regenerative chatter. Through updating a numerical solution scheme (NSS), a fast prediction method is proposed in this paper. Firstly, a NSS is constructed by combining the Lagrange polynomial and Euler's method. Then, the solution of the differential equations described the milling process is transformed into the initial-value problem of the equation which is expressed by the built NSS over each small discrete time interval. Subsequently, the state transition matrix over one tooth passing period is established to predict the stability lobe diagram (SLD) via the Floquet theory. Finally, the computational performances of the proposed method are verified by the single and two DOF dynamic models. Compared with the complete discretization scheme, the computational accuracy and efficiency of the proposed method are increased by 2.69 times and 2.01 times, respectively. The proposed method reduces the computational accuracy by 2.16 times in comparison to the first-order full-discretization method, but it increases the computational efficiency by 2.2 times.

Keywords Stability prediction · Lagrange polynomial · Euler's method · Stability lobe diagram · Mean relative mean

1 Introduction

Milling chatter is a detrimental phenomenon, which can seriously affect the machined efficiency and precision [1]. The stability prediction is usually used to find the suitable cutting parameters to suppress the chatter [2]. The dynamic model of the milling system considering the regenerative effect is generally characterized as the delayed differential equations (DDEs). From the aspect of solving form of the DDEs, various methods, such as the direct integration, numerical integration, and numerical iteration ones, have been proposed.

By using the direct integration scheme [3], the full-discretization method (FDM) was proposed to predict the

stability boundaries, where both the system state and time-delay terms of the DDEs were discretized simultaneously [4]. Compared with the semi-discretization method (SDM) [5], the computational efficient and accuracy of the FDM was better. With the aim to further improve the FDM, multiple interpolation schemes, mainly including the Lagrange polynomial, Newton polynomial, and Hermite polynomial, were introduced to approximate the delayed term or the system state term, thereby building the second-order or third-order FDMs [6–12]. Furthermore, the fourth and fifth order methods were proposed to further increase the accuracy of the stability prediction [13]. Even though the computational precision can be increased using these higher-order interpolation polynomials, the corresponding computational time is also increased obviously.

To overcome this bottleneck, the numerical integration schemes are introduced. Based on the integral equation built in the discretization method, the classical numerical integral formulas are used to estimate the corresponding integral term, thus decreasing the time cost. The Newton-Cotes and Gauss formulas were proposed to obtain the stability lobes [14, 15]. The Simpson method was studied to predict the milling stability [16], which showed the higher accuracy and efficiency compared with the FDM. Then, Ozoegwu

✉ Yan Xia
yxia1220@foxmail.com

¹ School of Mechanical Engineering, Qilu University of Technology (Shandong Academy of Sciences), Jinan 250353, China

² Shandong Institute of Mechanical Design and Research, Jinan 250031, China

³ Key Laboratory of High Efficiency and Clean Mechanical Manufacture, Ministry of Education, School of Mechanical Engineering, Shandong University, Jinan, 250061, China

et al. [17] extended the numerical integration method to the third and fourth order vector numerical integration schemes, and the higher computational accuracy was obtained. Subsequently, the Lagrange interpolation scheme and Simpson interpolation formula were introduced to update the numerical integration method, improving the predicted performance of the milling stability [18, 19]. To conduct the state transition matrix efficiently, other numerical schemes were consecutively proposed, such as the Adams-Moulton-based method [20], the Gaussian quadrature-based method [21], the Chebyshev-wavelet-based approach [22], and the Adams-Bashforth method [23],

Based on Euler's method, Li et al. [24] explored a complete discretization scheme (CDS) to predict the chatter stability, in which the system state, time delay, periodic coefficient, and the differential terms of the DDEs were discretized simultaneously. The numerical iteration method is introduced in the CDS to solve the DDEs, which is different from the above direct integration and numerical integration methods. Besides the milling operation, the CDS was applied to analyze the chatter stability of the orthogonal turn-milling process [25]. In order to increase the computational accuracy of the CDS, the periodic coefficient term was estimated by the linear interpolation [26]. Then, the classical Runge–Kutta method was introduced to improve the CDS, achieving the milling stability prediction [27]. Due to the brief form of the iteration equation, the time cost is decreased by using the numerical iteration method in contrast to the FDM.

Even though Euler's method can be used to construct the iteration equation to achieve the chatter stability, the computational accuracy of the corresponding method is lower due to the limit of the truncation error of Euler's formula. To improve the computational performance of the prediction method based on the Euler's formula, this paper updated a stability prediction method by introducing the numerical solution scheme (NSS). In this work, based on Euler's formula, the parabolic interpolation is introduced to construct the NSS in Section 2. Then, the algorithm of the milling stability prediction is constructed using the NSS in Section 3. The single and two DOF milling systems are used to verify the effectiveness for the proposed predicted method in Section 4. Finally, Section 5 concludes with some conclusions.

2 Construction of the numerical solution scheme

Suppose that $f(t)$ is a continuous function, whose values at the discrete points t_i , t_{i+1} , and t_{i+2} are $f(t_i)$, $f(t_{i+1})$, and $f(t_{i+2})$, respectively. According to the second-order Lagrange polynomial, the $f(t)$ at the interval $[t_i, t_{i+2}]$ can be expressed by:

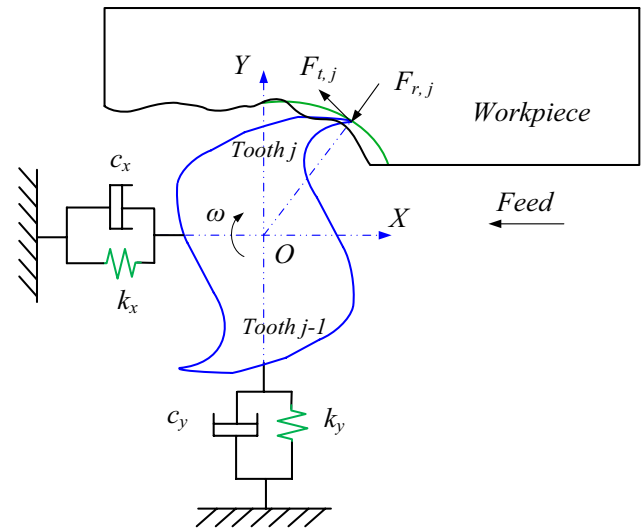


Fig. 1 Dynamic model of the two degrees of freedom (DOF) milling process [18]

$$f(t) \approx L_2(t) = \frac{(t-t_{i+1})(t-t_{i+2})}{2h^2} f(t_i) - \frac{(t-t_i)(t-t_{i+2})}{h^2} f(t_{i+1}) + \frac{(t-t_i)(t-t_{i+1})}{2h^2} f(t_{i+2}) \quad (1)$$

where the interval length $h = t_{i+1} - t_i = t_{i+2} - t_{i+1}$.

Through integrating on the two sides of Eq. (1) over the interval $[t_i, t_{i+1}]$, thus Eq. (2) can be obtained as

$$\int_{t_i}^{t_{i+1}} f(t) dt \approx \frac{h}{12} [5f(t_i) + 8f(t_{i+1}) - f(t_{i+2})] \quad (2)$$

Additionally, assuming that the $f(t)$ is the derivative of function $x(t)$, then, the relation between them can be expressed by

$$f(t) = \dot{x}(t) \quad (3)$$

Based on Euler's method, the solution of $x(t)$ over the interval $[t_i, t_{i+1}]$ can be expressed by

$$\int_{t_i}^{t_{i+1}} f(t) dt = x(t_{i+1}) - x(t_i) \quad (4)$$

Substituting Eq. (2) into Eq. (4), the solution of Eq. (4) can be approximated as

$$x(t_{i+1}) \approx x(t_i) + \frac{h}{12} [5f(t_i) + 8f(t_{i+1}) - f(t_{i+2})] \quad (5)$$

3 Calculation algorithm for the chatter stability prediction

Considering the regenerative chatter, the dynamic model for the milling system in Fig. 1 can be expressed by the following delayed differential equation:

$$M\ddot{q}(t) + C\dot{q}(t) + Kq(t) = wK_c(t)[q(t-T) - q(t)] \quad (6)$$

where \mathbf{M} , \mathbf{C} , and \mathbf{K} are the mass matrix, damping matrix, and stiffness matrix, respectively. $\mathbf{K}_c(t)$ is the periodic coefficient matrix, w is the axial cutting depth, $\mathbf{q}(t)$ is the modal coordinate, and T is the time period.

Introduce the notation $\mathbf{p}(t)$ and $\mathbf{x}(t)$:

$$\mathbf{p}(t) = M\dot{\mathbf{q}}(t) + C\mathbf{q}(t)/2, \mathbf{x}(t) = [\mathbf{q}(t)\mathbf{p}(t)]^T \quad (7)$$

Then, Eq. (6) can be transformed into the state-space form.

$$\dot{\mathbf{x}}(t) = \mathbf{A}\mathbf{x}(t) + \mathbf{B}(t)[\mathbf{x}(t-T) - \mathbf{x}(t)] \quad (8)$$

where

$$\mathbf{A} = \begin{bmatrix} -M^{-1}C/2 & M^{-1} \\ CM^{-1}C/4 - K & -CM^{-1}/2 \end{bmatrix}, \mathbf{B}(t) = \begin{bmatrix} 0 & 0 \\ wK_c(t) & 0 \end{bmatrix} \quad (9)$$

where \mathbf{A} refers to the constant coefficient matrix and $\mathbf{B}(t)$ stands for the periodic coefficient matrix with $\mathbf{B}(t) = \mathbf{B}(t+T)$.

Further, introduce the notation $\mathbf{C}(t)$ and $\mathbf{D}(t)$:

$$\mathbf{C}(t) = \mathbf{A} - \mathbf{B}(t), \mathbf{D}(t) = \mathbf{C}(t)\mathbf{x}(t) + \mathbf{B}(t)\mathbf{x}(t-T) \quad (10)$$

Thus, Eq. (8) can be rewritten as

$$\dot{\mathbf{x}}(t) = \mathbf{D}(t) \quad (11)$$

According to Eqs. (3) and (5), the solution of Eq. (11) can be expressed by

$$\mathbf{x}(t_{i+1}) = \mathbf{x}(t_i) + \frac{h}{12} [5\mathbf{D}(t_i) + 8\mathbf{D}(t_{i+1}) - \mathbf{D}(t_{i+2})] \quad (12)$$

where the time point $t_{i+1} = t_i + h$ and the time interval $h = T/m$, where m is the discrete number.

Due to the periodic nature of the milling system, the value $\mathbf{x}(t_1)$ at the time point t_1 can adopt the following expression:

$$\mathbf{x}(t_1) = \mathbf{x}(t_{m+1} - T) \quad (13)$$

At the time point t_2 , that is $i = 1$, the value $\mathbf{x}(t_2)$ can be given from Eq. (12) by

$$\mathbf{x}(t_2) = \mathbf{x}(t_1) + \frac{h}{12} [5\mathbf{D}(t_1) + 8\mathbf{D}(t_2) - \mathbf{D}(t_3)] \quad (14)$$

At other time point t_i ($i = 2, 3, \dots, m-1$), $\mathbf{x}(t_i)$ can be expressed by

$$\mathbf{x}(t_{i+1}) = \mathbf{x}(t_i) + \frac{h}{12} [5\mathbf{D}(t_i) + 8\mathbf{D}(t_{i+1}) - \mathbf{D}(t_{i+2})] \quad (15)$$

However, when $i = m$, $\mathbf{x}(t_i)$ cannot be described by Eq. (12) directly since $\mathbf{D}(t_{m+2})$ does not exist and can be obtained from the trapezoidal formula by [14, 18]

$$\mathbf{x}(t_{i+1}) = \mathbf{x}(t_i) + \frac{h}{2} [\mathbf{D}(t_i) + \mathbf{D}(t_{i+1})] \quad (16)$$

According to Eqs. (13)–(16), the discrete map of the system can be obtained as

$$\mathbf{R} \begin{bmatrix} \mathbf{x}(t_1) \\ \mathbf{x}(t_2) \\ \vdots \\ \mathbf{x}(t_{m+1}) \end{bmatrix} = \mathbf{S} \begin{bmatrix} \mathbf{x}(t_1 - T) \\ \mathbf{x}(t_2 - T) \\ \vdots \\ \mathbf{x}(t_{m+1} - T) \end{bmatrix} \quad (17)$$

with

$$\mathbf{R} = \begin{bmatrix} 0 & & & & \\ -(I + \frac{5h}{12}C(t_1)) & (I - \frac{2h}{3}C(t_2)) & \frac{h}{12}C(t_3) & & \\ & \ddots & \ddots & \ddots & \\ & & -(I + \frac{5h}{12}C(t_{m-1})) & (I - \frac{2h}{3}C(t_m)) & \frac{h}{12}C(t_{m+1}) \\ 0 & & & -(I + \frac{h}{2}C(t_m)) & (I - \frac{h}{2}C(t_{m+1})) \end{bmatrix} \quad (18)$$

$$\mathbf{S} = \begin{bmatrix} 0 & & & & \\ \frac{5h}{12}B(t_1) & \frac{2h}{3}B(t_2) & -\frac{h}{12}B(t_3) & & \\ & \ddots & \ddots & \ddots & \\ & & \frac{5h}{12}B(t_{m-1}) & \frac{2h}{3}B(t_m) & -\frac{h}{12}B(t_{m+1}) \\ 0 & & & \frac{h}{2}B(t_m) & \frac{h}{2}B(t_{m+1}) \end{bmatrix}$$

Then, the state transition matrix Φ on one time period is obtained by

$$\Phi = \mathbf{R}^{-1}\mathbf{S} \quad (19)$$

Lastly, the stable state for the milling system can be determined through identifying the eigenvalue of Φ according to the Floquet theory.

4 Verification and comparison

In order to verify the computational efficiency and precision for the proposed numerical integral Euler's method (NIEM), the comparisons for the SLD prediction in the single and two DOF milling systems using the NIEM, the FDM [4], and the CDS [24] are analyzed in detail. As a

Table 1 System parameters

Term	Notation	Value
Natural frequency	ω_n	922 Hz
Damping ratio	ζ	1.1%
Modal mass	m_t	0.03993 kg
Cutting force coefficients	K_t	$6 \times 10^8 \text{ N/m}^2$
	K_n	$2 \times 10^8 \text{ N/m}^2$
Tooth number	N	2

numerical iteration method, the computational accuracy of the CDS is limited by the truncation error of Euler's formula. The comparison between the CDS and the NIEM is to show whether the NIEM can improve the computational accuracy or not. Due to the introduction of the interpolating polynomial, the FDM generally has high computational accuracy but will lose the relative computational efficiency. The comparison between the CDS and the FDM is to demonstrate whether the NIEM can improve the computational efficiency or not. The corresponding coefficient matrixes in Eq. (9) are given in Appendix 1. The system parameters are listed in Table 1, which are consistent with those in Ref. [4, 24]. In the meantime, the MATLAB codes are operated in a personal computer (Intel (R) Core (TM) i5, 2.3 GHz, and 6 GB).

4.1 Single DOF milling process

For the single DOF milling model, the system parameters in Table 1 are used to calculate the SLDs. The discrete number m is selected as 80. Under down milling operation, the SLDs with the different radial depth of cut ratios are obtained using the proposed NIEM, the CDS [24], and the FDM [4] respectively, as shown in Fig. 2. The exact stability boundaries (ESB) from the FDM with $m=200$ are presented to provide a reference in black color.

From Fig. 2, it can be found that the SLDs obtained from the NIEM are more close to the ideal lobes, than the curves determined from the CDS. It shows that the computational accuracy of the NIEM is higher than that of the CDS. In order to quantitatively demonstrate the computational advantage of the NIEM, the mean relative error (MRE) is introduced. For example, when w/D is 0.05 in Fig. 2a, under six rotational speeds ($\Omega = 5000 \text{ rpm}$, 6000 rpm , 7000 rpm , 8000 rpm , 9000 rpm , and $10,000 \text{ rpm}$), the absolute relative errors between the two SLDs from the NIEM and the ESB are 0.23, 0.07, 0.06, 0.06, 0.23, and 0.03. Then, the MRE of the NIEM under $w/D=0.05$ is 0.113. Similarly, under the different w/D and the different predicted methods, the corresponding MREs can be obtained, which are listed in Table 2 and are illustrated in Fig. 3. Figure 3 presents that the MREs of the CDS is the largest, followed by the NIEM,

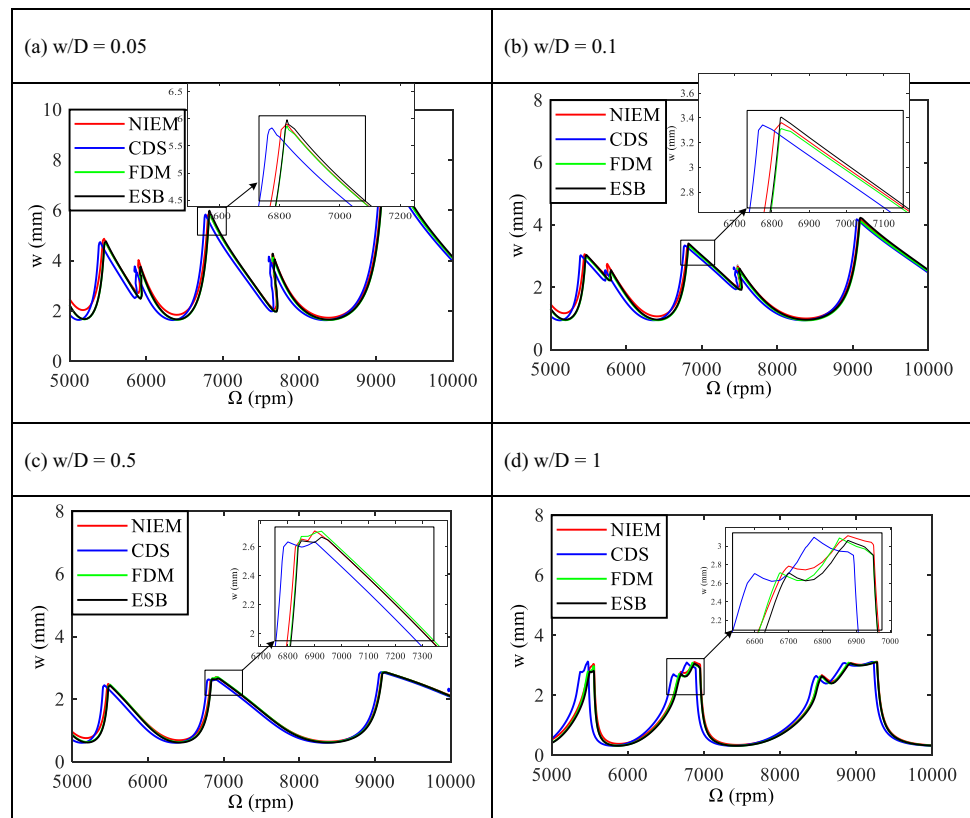
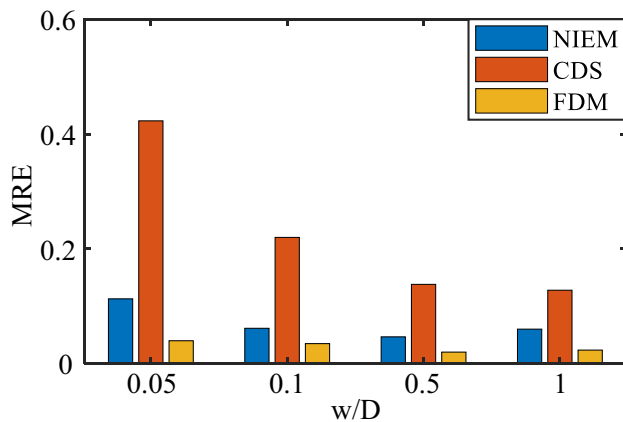
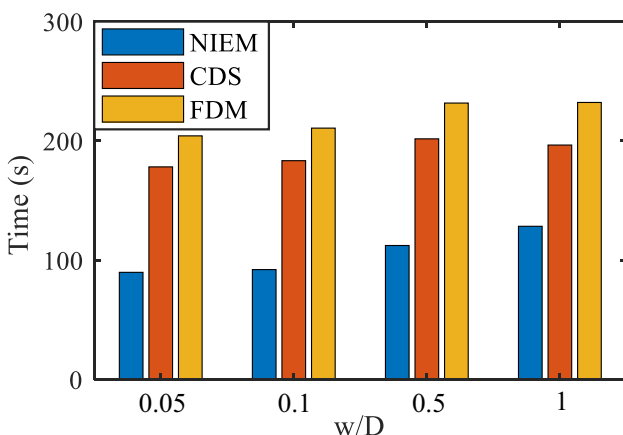
Fig. 2 Comparison of the SLDs with different w/D in the single DOF milling system

Table 2 Mean relative error of the different methods with a single DOF model

Methods	w/D			
	0.05	0.1	0.5	1
NIEM	0.113	0.062	0.047	0.060
CDS	0.423	0.220	0.138	0.128
FDM	0.04	0.035	0.020	0.024

**Fig. 3** MREs of the different predicted method under different w/D **Table 3** Computational time of the different methods with single DOF model(s)

Methods	w/D			
	0.05	0.1	0.5	1
NIEM	89.8	92.1	112.3	128.4
CDS	178.2	183.4	201.7	196.5
FDM	204.2	210.7	231.7	232.2

**Fig. 4** Time cost from the NIEM, CDS, and FDM with different w/D

and the FDM is the smallest. It reveals that the computational accuracy of the NIEM is higher than that of CDS, but it is lower than that of the FDM.

When calculating the SLDs in Fig. 2, the corresponding computational time is listed in Table 3 and is depicted in Fig. 4. As shown in Fig. 4, when the w/D increases, the time cost increases among the three methods. However, under the same value of w/D , the computation time using the NIEM is always much less than those of the CDS and FDM, which shows that the improvement of the computational efficiency for the proposed NIEM.

Then, based on the data in Tables 2 and 3, the comparisons of the computational accuracy and efficiency between the different methods are carried out, such as NIEM/CDS and NIEM/FDM, as shown in Table 4. Compared with the CDS, the accuracy and efficiency of the NIEM are increased by 3.1 times and 1.83 times, respectively. The NIEM losses the accuracy by 2.36 times but improves the efficiency by 2.11 times, compared with the FDM.

4.2 Two DOF milling process

For the two DOF milling model, the used parameters are listed in Table 1 as well. Similarly, the discrete number m is still selected as 80. With the different w/D , the SLDs are calculated using the NIEM, CDS, and FDM, respectively. As shown in Fig. 5, the curves from the CDS are farther away from the ideal lobes, and the lobes from the NIEM are near to the ideal SLDs.

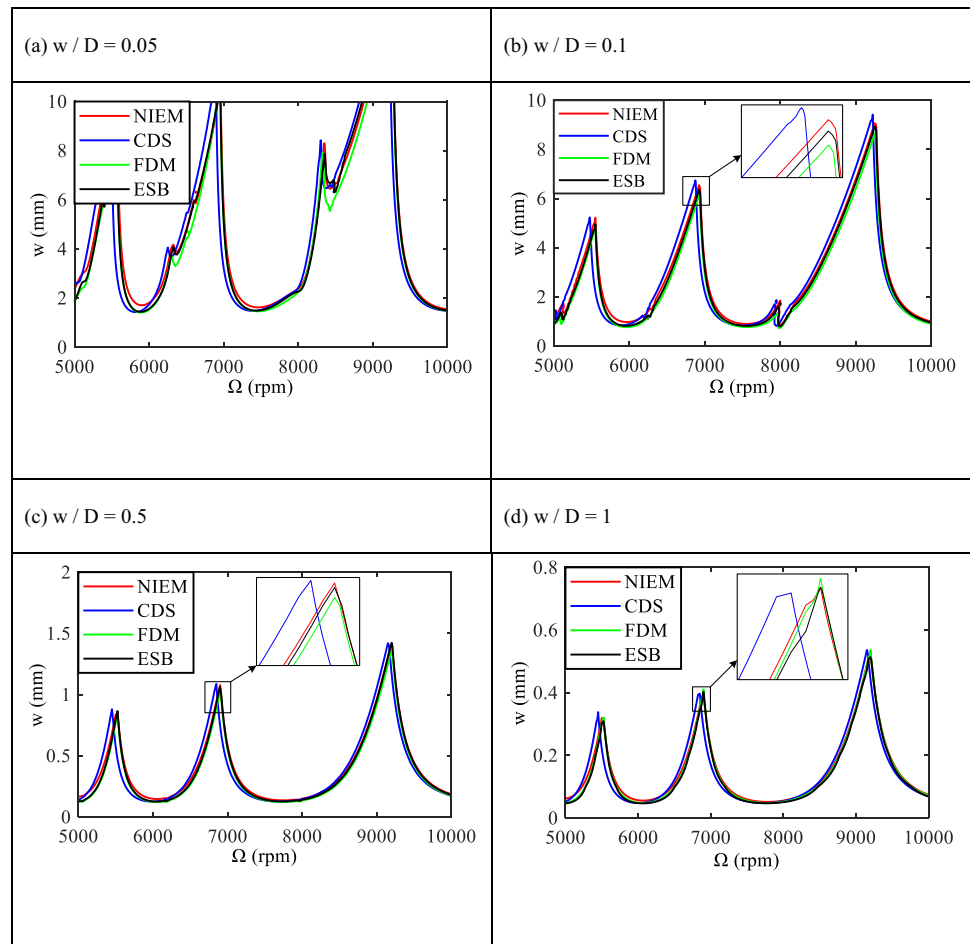
In order to further compare the computational accuracy among the three methods, the MREs are also calculated and are listed in Table 5. The data of Table 5 is illustrated in Fig. 6. From Fig. 6, it can be found that under the same w/D , the CDS has the highest MRE, which shows the worst computational accuracy. Apparently, the FDM has the best accuracy among the three methods.

Furthermore, the runtime of the obtained SLDs in Fig. 5 is listed in Table 6, where Fig. 7 demonstrates these data graphically. From Fig. 7, it clearly shows that under the same w/D , the computational time of the FDM is the highest, whereas that from the NIEM is the smallest. The proposed NIEM shows the better computational efficiency.

In the two DOF milling models, the comparisons between the two different methods including NIEM/CDS and NIEM/FDM are performed in terms of the computational accuracy and efficiency, which can be seen in Table 7. The comparison results are similar to those in Table 4 of the single DOF milling system. The NIEM can increase the computational accuracy and efficiency with 2.28 times and 2.19 times, comparing to the CDS. In comparison with the FDM, the NIEM still decreased the accuracy by 1.96 times, but it increases the efficiency by 2.29 times.

Table 4 Comparisons between the different methods with single DOF model

Methods	Items	w/D				Mean
		0.05	0.1	0.5	1	
NIEM/CDS	Accuracy	3.74	3.57	2.95	2.13	3.10
	Efficiency	1.98	1.99	1.80	1.53	1.83
NIEM/FDM	Accuracy	-2.83	-1.76	-2.32	-2.54	-2.36
	Efficiency	2.27	2.29	2.06	1.80	2.11

Fig. 5 Comparison of the SLDs with different w/D in the two DOF milling system

4.3 Comparison analysis with the different discrete number

Table 5 Mean relative error of the different methods with two DOF models

Methods	w/D			
	0.05	0.1	0.5	1
NIEM	0.294	0.147	0.017	0.009
CDS	0.572	0.367	0.044	0.018
FDM	0.027	0.112	0.013	0.003

To further verify the computational performance for the proposed method, the SLDs with the different m for the single DOF milling system are calculated using the NIEM and CDS respectively, where w/D is chosen as 1. The obtained SLDs are shown in Fig. 8. When $m=40$, both of the SLDs from the NIEM and CDS are far away from the ideal curve at the low speed range, but the stability lobes from the NIEM at the higher speed are faster close to the exact SLD than that

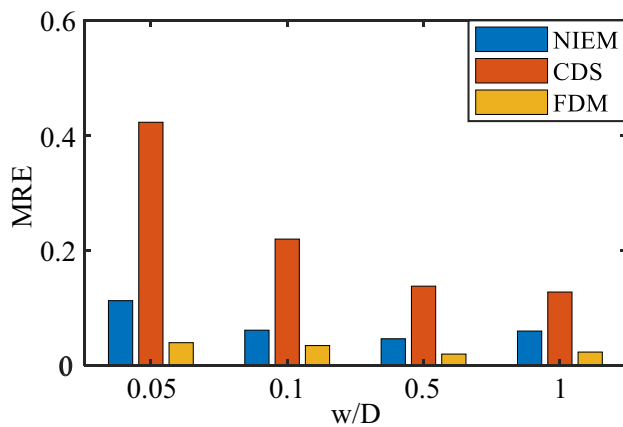


Fig. 6 MREs of the different predicted method under different w/D

Table 6 Computational time of the different methods with two DOF models

Methods	w/D			
	0.05	0.1	0.5	1
NIEM	268.8	276.4	314.2	441.4
CDS	630.9	650.9	686.7	820.3
FDM	681.6	706.7	739.5	869.2

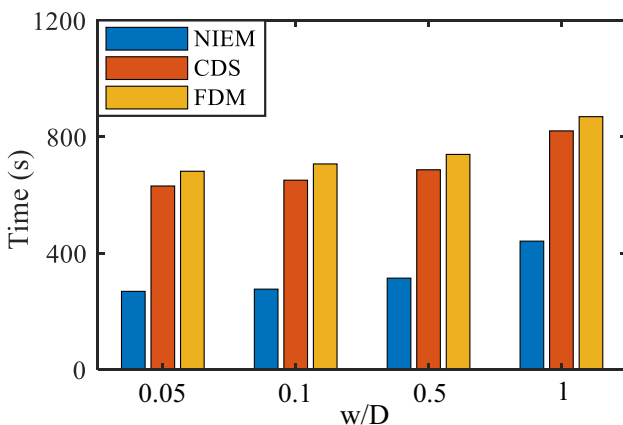


Fig. 7 Time cost from the NIEM, CDS, and FDM with different w/D

Table 7 Comparisons between the different methods with single DOF model

Methods	Items	w/D				Mean
		0.05	0.1	0.5	1	
NIEM/CDS	Accuracy	1.95	2.50	2.65	2.01	2.28
	Efficiency	2.35	2.35	2.19	1.86	2.19
NIEM/FDM	Accuracy	-10.9	-1.31	-1.28	-3.3	-1.96
	Efficiency	2.54	2.56	2.35	1.97	2.29

from the CDS. As m further increases, the SLDs obtained from the NIEM are always more accurate than those from the CDS. Especially, when m is equal to 200, the lobes from the NIEM almost coincided with the exacted curves, whereas there exists an obvious difference between the lobes from the CDS and the ESB.

From the time-consuming point of view, Table 8 shows that the computational time will be increased obviously when m increases. When $m = 40$, the runtime from the NIEM, CDS, and FDM is 47.3 s, 50.5 s, and 66.7 s, respectively, where the differences among the time cost are minor. However, as m increases, the differences are growing rapidly. In order to compare with the runtime intuitively, the computational time using the three methods is plotted as shown in Fig. 9. From the figure, it can be found that the runtime of the NIEM is always less than those of the other two. Therefore, compared with the CDS, the proposed method has the better computational precision and efficiency.

5 Conclusions

A fast prediction method for milling stability is built in this work. In order to solve the initial-value problem of the differential equations for the milling system, a numerical solution scheme (NSS) is construction based on the Lagrange integral formula and Euler's method. Then, the NSS is used to build the solution algorithm for the dynamic equations of the milling system. On this basis, the state transition matrix over one time period is derived and thus is used to calculate the chatter stability according to the Floquet theory. In comparison with the CDS, the proposed method can effectively increase the computational accuracy and efficiency, where the average improvements are 2.69 and 2.01 times, respectively. Compared with the FDM, the computational accuracy of the proposed method is averagely reduced by 2.16 times, but the corresponding efficiency is averagely increased by 2.2 times.

Apparently, the introduced Euler's formula limits the computational accuracy of the proposed method. Therefore, under the premise of ensuring efficiency, the proposed method should be further studied in the future.

Fig. 8 Comparison of the SLDs for the NIEM and the CDS with the different m

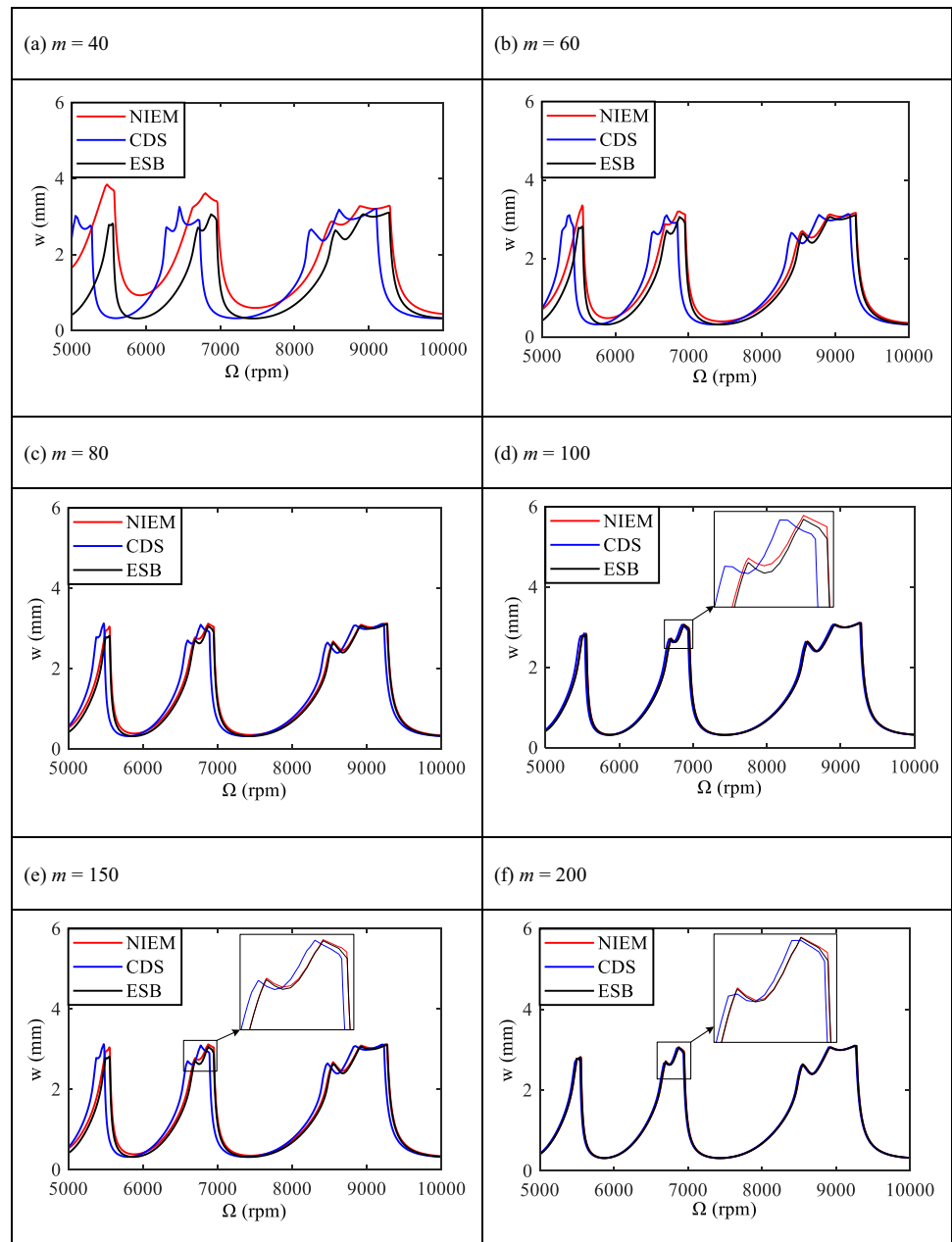


Table 8 Computation time with different m (s)

Methods	m					
	40	60	80	100	150	200
NIEM	47.3	88.3	128.4	209.3	514.4	947.8
CDS	50.5	107.4	196.5	341.7	1064.8	2910.1
FDM	66.7	134.2	232.2	402.1	1221.3	3185.7

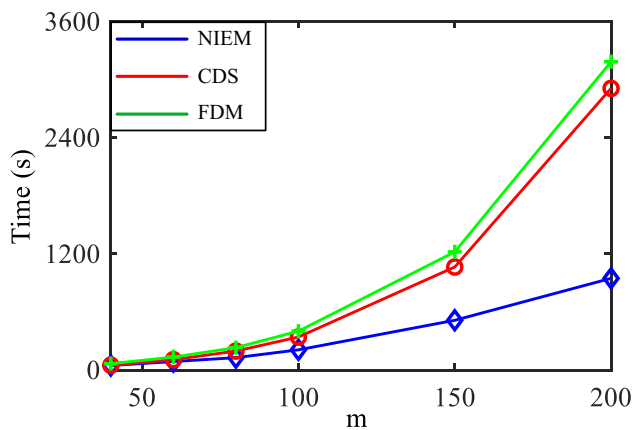


Fig. 9 Time cost from the NIEM, CDS, and FDM with different m

Appendix 1 Coefficient matrixes for single and two DOF milling systems

The coefficient matrixes for the single DOF milling system can be described as

$$\mathbf{A} = \begin{bmatrix} -\xi\omega_n & \frac{1}{m_t} \\ (\xi^2 - 1)m_t\omega_n^2 & -\xi\omega_n \end{bmatrix}$$

$$\mathbf{B}(t) = \begin{bmatrix} 0 & 0 \\ wh(t) & 0 \end{bmatrix}$$

where $h(t)$ is the cutting force coefficient.

The coefficient matrixes for the two DOF milling system can be described as

$$\mathbf{A} = \begin{bmatrix} -\mathbf{M}^{-1}\mathbf{C}/2 & \mathbf{M}^{-1} \\ \mathbf{CM}^{-1}\mathbf{C}/4 - \mathbf{K} & -\mathbf{CM}^{-1}/2 \end{bmatrix}$$

$$\mathbf{B}(t) = \begin{bmatrix} 0 & 0 & 0 & 0 \\ 0 & 0 & 0 & 0 \\ wh_{xx}(t) & wh_{xy}(t) & 0 & 0 \\ wh_{yx}(t) & wh_{yy}(t) & 0 & 0 \end{bmatrix}$$

with

$$\mathbf{M} = \begin{bmatrix} m_t \\ m_t \end{bmatrix} \quad \mathbf{C} = \begin{bmatrix} 2m_t\xi \\ 2m_t\xi \end{bmatrix} \quad \mathbf{K} = \begin{bmatrix} m_t\omega_n^2 \\ m_t\omega_n^2 \end{bmatrix}$$

Author contribution Yan Xia, Yi Wan, and Guosheng Su contributed to the conceptualization and methodology; Yan Xia, Peirong Zhang, and Jin Du performed the investigation and analysis; Yan Xia wrote the manuscript.

Funding This research was funded by the National Natural Science Foundation of China (Grant No. 51975336), Key Research and Development Program of Shandong Province (Grant No. 2020JMRH0202), the Natural Science Foundation of Shandong Province (Grant No. ZR2022QE241), the New Old Energy conversion Major Industrial

Tackling Project of Shandong Province (Grant No. 2021–13), and Key Research and Development Program of Jining City (2021DZP005).

Data availability The data can be available from the corresponding author.

Code availability Not applicable.

Declarations

Conflict of interest The authors declare that they have no conflict of interest.

References

- Totis G, Albertelli P, Torta M, Sortino M, Monno M (2017) Upgraded stability analysis of milling operations by means of advanced modeling of tooling system bending. *Int J Mach Tools Manuf* 113:19–34
- Yang Y, Zhang WH, Ma YC, Wan M (2016) Chatter prediction for the peripheral milling of thin-walled workpieces with curved surfaces. *Int J Mach Tools Manuf* 109:36–48
- Gu YX, Chen BS, Zhang HW, Guan ZQ (2001) Precise time-integration method with dimensional expanding for structural dynamic equations. *AIAA J* 39(12):2394–2399
- Ding Y, Zhu LM, Zhang XJ, Ding H (2010) A full-discretization method for prediction of milling stability. *Int J Mach Tools Manuf* 50(5):502–509
- Inserperger T, Stépán G (2004) Updated semi-discretization method for periodic delay-differential equations with discrete delay. *Int J Numer Meth Eng* 61:117–141
- Ding Y, Zhu LM, Zhang XJ, Ding H (2010) Second-order full-discretization method for milling stability prediction. *Int J Mach Tools Manuf* 50(10):926–932
- Quo Q, Sun YW, Jiang Y (2012) On the accurate calculation of milling stability limits using third-order full-discretization method. *Int J Mach Tools Manuf* 62:61–66
- Liu YL, Zhang DH, Wu BH (2012) An efficient full-discretization method for prediction of milling stability. *Int J Mach Tools Manuf* 63:44–48
- Liu YL, Fischer A, Eberhard P, Wu BH (2015) A high-order full-discretization method using Hermite interpolation for periodic time-delayed differential equations. *Acta Mech Sin* 31(03):406–415
- Qin CJ, Tao JF, Liu CL (2019) A novel stability prediction method for milling operations using the holistic-interpolation scheme. *Proc IMechE, Part C: J Mech Eng Sci* 233(13): 4463–4475
- Ji YJ, Wang XB, Liu ZB, Wang HJ, Wang KJ, Wang DQ (2019) Stability prediction of five-axis ball-end finishing milling by considering multiple interaction effects between the tool and workpiece. *Mech Syst Signal Process* 131:261–287
- Ji YJ, Wang LY, Song Y, Wang HJ, Liu ZB (2022) Investigation of robotic milling chatter stability prediction under different cutter orientations by an updated full-discretization method. *J Sound Vib* 536:117150
- Ozoegwu CG, Omenyi SN, Ofochebe SM (2015) Hyper-third order full-discretization methods in milling stability prediction. *Int J Mach Tools Manuf* 92:1–9
- Ding Y, Zhu LM, Zhang XJ, Ding H (2011) Numerical integration method for prediction of milling stability. *J Manuf Sci Eng* 133(3):1–9

15. Li WT, Wang LP, Yu G (2020) An accurate and fast milling stability prediction approach based on the Newton-Cotes rules. *Int J Mech Sci* 177:105469
16. Zhang Z, Li HG, Meng G, Liu C (2015) A novel approach for the prediction of the milling stability based on the Simpson method. *Int J Mach Tools Manuf* 99:43–47
17. Ozoegwu CG (2016) High order vector numerical integration schemes applied in state space milling stability analysis. *Appl Math Comput* 273:1025–1040
18. Xia Y, Wan Y, Luo XC, Liu ZQ, Song QH (2021) An improved numerical integration method to predict the milling stability based on the Lagrange interpolation scheme. *Int J Adv Manuf Technol* 116(7):2111–2123
19. Xia Y, Wan Y, Su GS, Du J, Zhang PR, Xu CH (2022) An improved numerical integration method for prediction of milling stability using the Lagrange-Simpson interpolation scheme. *Int J Adv Manuf Technol* 120(11–12):8105–8115
20. Tao JF, Qin CJ, Liu CL (2017) Milling stability prediction with multiple delays via the extended Adams-Moulton-based method. *Math Probl Eng* 2017:1–15
21. Yang Y, Yuan JW, Tie D, Wan M, Zhang WH (2023) An efficient and accurate chatter prediction method of milling processes with a transition matrix reduction scheme. *Mech Syst Signal Process* 182:109535
22. Qin CJ, Tao JF, Shi HT, Xiao DY, Li BC, Liu CL (2020) A novel Chebyshev-wavelet-based approach for accurate and fast prediction of milling stability. *Precis Eng* 62:244–255
23. Dun YC, Zhu LD, Wang SH (2020) Multi-modal method for chatter stability prediction and control in milling of thin-walled workpiece. *Appl Math Model* 80:602–624
24. Li MZ, Zhang GJ, Huang Y (2013) Complete discretization scheme for milling stability prediction. *Nonlinear Dyn* 71(1):187–199
25. Sun T, Qin LF, Fu YC, Hou JM (2019) Chatter stability of orthogonal turn-milling analyzed by complete discretization method. *Precis Eng* 56:87–95
26. Xie QZ (2016) Milling stability prediction using an improved complete discretization method. *Int J Adv Manuf Technol* 83(5):815–821
27. Lv SJ, Zhao Y (2021) Stability of milling process with variable spindle speed using Runge–Kutta-based complete method. *Math Probl Eng* 2021:1–10

Publisher's note Springer Nature remains neutral with regard to jurisdictional claims in published maps and institutional affiliations.

Springer Nature or its licensor (e.g. a society or other partner) holds exclusive rights to this article under a publishing agreement with the author(s) or other rightsholder(s); author self-archiving of the accepted manuscript version of this article is solely governed by the terms of such publishing agreement and applicable law.